Fourth-generation quarks and leptons

V. Barger, H. Baer, and K. Hagiwara
Physics Department, University of Wisconsin, Madison, Wisconsin 53706

R. J. N. Phillips
Rutherford Appleton Laboratory, Chilton, Didcot, Oxon, England
(Received 30 January 1984; revised manuscript received 14 May 1984)

We study the production, decay, and detection of fourth-generation quarks and leptons at present and future hadron colliders. We use a plausible extension of the quark-mixing systematics of three generations. We consider a range of heavy-quark masses that include overlapping generations and superheavy quarks that decay to the W boson. One particularly intriguing possibility is a new charge $-\frac{1}{3}$ quark (v) with mass comparable to the t-quark mass. Hadronic $v\bar{v}$ production could exceed $t\bar{t}$ production, but there would be no substantial analog to the $W\to t\bar{b}$ source. The $v\to c$ decay would resemble $t\to b$ decay in many respects, except that the v lifetime is long and might be measurable with microvertex detectors. We discuss how the cluster transverse mass, the identification of b and c hadrons, and possible diffractive leading-particle effects might differentiate between v and t semileptonic-decay signals. Electroweak W^+W^- pair production is also evaluated as a benchmark with which superheavy-quark signals can be compared.

I. INTRODUCTION

The next immediate focus of $p\bar{p}$ collider research is the t quark,[1,2] now that the W and Z weak bosons have been discovered.[3] Systematic procedures have been proposed[4] for the separation of t-quark signals from other heavy-quark backgrounds and hopefully this will be accomplished in the near future. An equally important question is the possible existence of a fourth generation of quarks and leptons. In fact, viable experimental signatures have already been discussed for a heavy charged lepton[5] produced via $W\to L\nu$ decay and for a heavy sequential neutrino[6] produced via $Z\to\nu\bar{\nu}$ decay or $e^+e^-\to\nu\bar{\nu}$. In this paper we address the production, decay, and detection of fourth-generation quarks and leptons at present and future hadron colliders. Our considerations are based on a plausible extension of the empirical systematics of the quark mixing angles in the three-generation case. We consider various possibilities for the masses of the fourth-generation quarks, such as a fourth-generation $Q=-\frac{1}{3}$ quark with mass comparable to that of the t quark and also superheavy quarks that decay by W-boson emission. We also briefly present the rate for heavy-lepton production via a virtual W intermediate state, for the case that the L mass is comparable to or exceeds the W mass. Electroweak W^+W^- pair production is also evaluated as a benchmark with which superheavy-quark signals can be compared.

We shall denote the fourth-generation leptons by (ν_L,L) and the fourth-generation quarks by (a,v), where a and v have charges $(\frac{2}{3},-\frac{1}{3})$. This notation for fourth-generation quarks is suggested by the alphabetic labels used for the other quarks (viz., $a,b,c,d;s,t,u,v$).

A significant constraint on the a,v masses is found from radiative corrections to the quantity

$$\rho=\frac{G\ (\text{neutral current})}{G\ (\text{charged current})}\ ,$$

where $\rho=1+O(\alpha)$ in Weinberg-Salam theory. The contribution to ρ from the fourth-generation fermions is[7]

$$\Delta\rho=\frac{G_F}{8\sqrt{2}\pi^2}[3f(m_a,m_v)+f(m_\nu,m_L)] \tag{1}$$

with m_ν denoting the ν_L mass and

$$f(M,m)=M^2+m^2-\frac{2M^2m^2}{M^2-m^2}\ln\frac{M^2}{m^2}\ . \tag{2}$$

We note that the function $f(M,m)$ is bounded as

$$(M-m)^2\le f(M,m)\le\tfrac{4}{3}(M-m)^2\ . \tag{3}$$

The left equality applies when $m\ll M$ or $m\gg M$, while the right equality is obtained for a nearly degenerate doublet, $m\simeq M$.

The value of ρ found from deep-inelastic ν_μ and $\bar{\nu}_\mu$ scattering data is[8]

$$\rho=1.02\pm0.02\ .$$

With the one-loop radiative correction, the standard model (with three generations, $m_t=35$ GeV, and $M_{\text{Higgs}}=M_Z$ assumed) predicts[8,9]

$$\rho=1.000\,52\ .$$

Hence the fourth-generation contribution to ρ is bounded by

$$\Delta\rho<0.04 \tag{4}$$

at the one-standard-deviation level. Thus, from Eqs. (1) and (4) we find the constraint

$$(m_v-m_a)^2+\tfrac{1}{3}(m_\nu-m_L)^2<(310\ \text{GeV})^2\ . \tag{5}$$

The factor of $\frac{1}{3}$ is replaced by $\frac{1}{4}$ if $m_\nu \ll m_L$. As long as the a and v masses are sufficiently degenerate, their absolute masses are unrestricted by $\Delta\rho$.

If the absolute masses are sufficiently high, then the weak interaction among heavy particles becomes strong and perturbation theory breaks down. With the assumption that perturbation theory is not to violate partial-wave unitarity, the following bounds on fourth-generation masses obtain:[10]

$$\begin{aligned} &m_a < 500 \text{ GeV} \quad (m_a \simeq m_v) , \\ &m_a < 700 \text{ GeV} \quad (m_a \gg m_v) , \\ &m_L < 900 \text{ GeV} \quad (m_L \simeq m_\nu) , \\ &m_L < 1000 \text{ GeV} \quad (m_L \gg m_\nu) . \end{aligned} \tag{6}$$

Should even heavier fermions exist, then all perturbation-theory estimates, including the one in Eq. (5) become suspect. There exist further model-dependent bounds on fermion masses motivated by vacuum stability[11] in the minimal Weinberg-Salam model or by the validity of perturbation theory in simple grand unification models,[12] some of which are more stringent than the bounds of Eq. (6).

It is interesting to note that some theoretical models have a heavy fermion. For example, if the normalization-group equations describing the evolution of couplings possess stable infrared fixed points, then a heavy-quark mass of order 100 GeV is predicted.[13] Also, in models with supersymmetry broken by radiative corrections a heavy sequential fermion with mass of order 60 GeV or more is necessary.[14]

In the following we consider fourth-generation masses which obey the bounds of Eqs. (5) and (6). Following the pattern of the first three generations, we assume throughout that $m_\nu \ll m_L$ and $m_v < m_a$.

Once particular a,v mass values are specified, the remaining degrees of freedom are the quark-mixing-matrix elements. In the three-generation case the mixing matrix is highly constrained by experiments, except for the CP-violating phase. Since we are at present concerned only with the strengths of decay transitions, we can ignore all CP-violating phases. The latest information on the matrix elements is derived[15] from B-decay measurements. The B lifetime[16] fixes $|U_{cb}| \sim 0.05$. The CESR limit[17]

$$\Gamma(b \to u)/\Gamma(b \to c) < 0.04$$

then gives $|U_{ub}| < 0.007$. Strange-particle decays and neutrino charm production determine[15] that $|U_{us}| \simeq |U_{cd}|$. These values suggest that the mixing matrix be symmetric.[18] With all experimental and unitarity constraints, and assuming symmetry, the magnitudes of the elements of the 3×3 matrix have the approximate form[15]

$$|U_{nm}| = \begin{array}{c} \begin{matrix} d & s & b \end{matrix} \\ \begin{bmatrix} 0.97 & 0.23 & <0.007 \\ 0.23 & 0.97 & 0.05 \\ <0.007 & 0.05 & 0.99 \end{bmatrix} \end{array} \begin{matrix} u \\ c \\ t \end{matrix} . \tag{7}$$

In the Kobayashi-Maskawa (KM) formalism, symmetry requires $\theta_2 = \theta_3$. Then, using the particle data Group conventions for the KM angles θ_i and phase δ, we find the following approximate relations:

$$\begin{aligned} &|U_{us}| \simeq \theta_1 , \\ &|U_{cb}| \simeq 2\theta_2 \sin(\tfrac{1}{2}|\delta|) , \\ &|U_{ub}| \simeq \theta_1\theta_2 \simeq \frac{\theta_1 |U_{cb}|}{2\sin(\frac{1}{2}|\delta|)} , \end{aligned} \tag{8}$$

where $\theta_1 \simeq 0.23$. Empirically we observe that

$$\begin{aligned} &|U_{cb}| \simeq \theta_1^2 , \\ &|U_{ub}| \lesssim \tfrac{1}{2}\theta_1^3 \simeq 2\theta_1^4 . \end{aligned} \tag{9}$$

Equation (8), based on a symmetric matrix, is compatible with the experimental limit on $|U_{ub}|/|U_{cb}|$ only if this limit is about saturated and $|\delta| \simeq \pi$. The nondiagonal elements of the symmetric 3×3 KM matrix can then be expressed as any one of the following numerically equivalent forms:

$$|U_{nm}| = (\tfrac{1}{2})^{n-m-1}\theta^{2n-m-2} , \tag{10a}$$

$$|U_{nm}| = (\tfrac{1}{2})^{n-m-1}\theta^{1/2(n-m)(n+m-1)} , \tag{10b}$$

$$|U_{nm}| = (2)^{n-m-1}\theta^{3n-2m-3} , \tag{10c}$$

$$|U_{nm}| = (2)^{n-m-1}\theta^{(n-m)(n-1)} \tag{10d}$$

for $n > m$. The diagonal elements are fixed by unitarity.

We now assume that the $|U_{nm}|$ forms of Eq. (10) generalize to the four-generation case. Equations (10a) and (10c) remain numerically equivalent; Eqs. (10b) and (10d) are equivalent in all elements but U_{ad}, which has no readily identifiable physics consequences anyway. Thus, we are left with two plausible distinct choices for the matrices, Eqs. (10a) and (10b), explicitly,

$$|U_{nm}| = \begin{array}{c} \begin{matrix} d & s & b & v \end{matrix} \\ \begin{bmatrix} 1- & \theta & \frac{1}{4}\theta^3 & \frac{1}{4}\theta^5 \\ \theta & 1- & \frac{1}{2}\theta^2 & \frac{1}{2}\theta^4 \\ \frac{1}{2}\theta^3 & \theta^2 & 1- & \theta^3 \\ \frac{1}{4}\theta^5 & \frac{1}{2}\theta^4 & \theta^3 & 1- \end{bmatrix} \end{array} \begin{matrix} u \\ c \\ b \\ a \end{matrix} \tag{11a}$$

and

$$|U_{nm}| = \begin{array}{c} \begin{matrix} d & s & b & v \end{matrix} \\ \begin{bmatrix} 1- & \theta & \frac{1}{2}\theta^3 & \frac{1}{4}\theta^6 \\ \theta & 1- & \theta^2 & \frac{1}{2}\theta^5 \\ \frac{1}{2}\theta^3 & \theta^2 & 1- & \theta^3 \\ \frac{1}{4}\theta^6 & \frac{1}{2}\theta^5 & \theta^3 & 1- \end{bmatrix} \end{array} \begin{matrix} u \\ c \\ t \\ a \end{matrix} . \tag{11b}$$

Here the diagonal values are slightly less than unity, as required by unitarity. The significant aspect of these mixing matrices is the increased suppression of transitions between different generations as the generation separation increases and as the generation mass increases. These are empirical facts for the first three generations, and Eqs.

(11) provide plausible extrapolation patterns. We anticipate that qualitative conclusions based on the suppression of cross-generational transitions will be valid, even though some details of the true 4×4 mixing matrix may differ from Eqs. (11).

For the weak decays of a and v, the principal decay branches, if energetically allowed, are

$$a\to v+W^+,\quad |U_{av}|\sim 1\,,$$
$$v\to t+W^-,\quad |U_{tv}|\sim\theta^3\,, \tag{12}$$

where the W bosons may be real or virtual, depending on the quark masses. An exception to Eq. (12) occurs if the third- and fourth-generation masses overlap, $m_v<m_t$. Then the v quark decays via

$$v\to c+W^-,\quad |U_{vc}|\sim\tfrac{1}{2}\theta^4 \text{ or } \tfrac{1}{2}\theta^5\,, \tag{13}$$

where the W^- is necessarily virtual. The distinctive aspect of this mode is the extreme mixing suppression, which would result in a long v-quark lifetime.

The decay widths of a and v quarks are evaluated in Sec. II, with special attention to the possibility of a long v lifetime. Hadronic and electroweak production cross sections of a and v quarks are given in Sec. III, while Sec. IV addresses distributions of decay particles.

Should the v mass be comparable to the t mass (the case of "overlapping quark generations"), considerable confusion could result in the identification of the decaying quark. The kinematic distributions of the decay fragments from v and t decays could be very similar; for example, $v\to ce\nu$ and $t\to be\nu$ differ only in their lepton distributions and in the quark jet (c or b) emitted in their decays. The $v\bar{v}$ production contribution might thereby masquerade as an enhanced source of $t\bar{t}$ events. Should the t-mass value obtained from $W\to t\bar{b}$ initiated events be different than that from supposedly $t\bar{t}$ events, that could indicate the existence of both t and v sources. Any $W\to a\bar{v}$ or $t\bar{v}$ contributions are likely to be negligible due to phase-space suppression and $W\to c\bar{v}$ is suppressed by mixing, but the hadronic $v\bar{v}$ production rate is comparable to $t\bar{t}$ if their masses are close. Section V addresses the important problem of distinguishing between t and v quarks in the case of overlapping quark generations. Finally, Sec. VI evaluates electroweak W^+W^- pair production as a benchmark for comparison with other processes. Our calculations are performed using Monte Carlo methods, with typically 5×10^4 shots giving accuracies of a few percent.

II. WEAK DECAYS OF a,v QUARKS

Consider the weak decay of a heavy quark

$$Q\to qW,\quad W\to F\bar{f}\,, \tag{14}$$

where the W may be real or virtual and $F\bar{f}$ are leptons. The matrix element for this transition is

$$\mathcal{M}=\frac{U_{Qq}M_W{}^2}{W^2-M_W{}^2+iM_W\Gamma_W}\frac{G}{\sqrt{2}}[\bar{u}(q)\gamma_\mu(1-\gamma_5)u(Q)]\times[\bar{u}(F)\gamma_\nu(1-\gamma_5)v(f)]\left[-g^{\mu\nu}+\frac{W^\mu W^\nu}{M_W{}^2}\right], \tag{15a}$$

where

$$G=\pi\alpha(W^2)/\sqrt{2}x_W(W^2)M_W{}^2 \tag{15b}$$

and four-momenta are denoted by particle labels. In later numerical evaluations of the decay widths we use $x_W(W^2)\simeq x_W(M_W{}^2)\simeq0.22$, $m_W=82$ GeV, and $\alpha(W^2)\simeq\alpha(M_W{}^2)\simeq\frac{1}{128}$. Squaring $\mathcal{M}$ and summing over spin states, we obtain

$$\sum|\mathcal{M}|^2=\frac{|U_{Qq}|^2M_W{}^4}{(W^2-M_W{}^2)^2+M_W{}^2\Gamma_W{}^2}\frac{G^2}{2}64\times\left\{4F\cdot q\,f\cdot Q+\frac{2}{M_W{}^2}[q^2(F^2Q\cdot f+f^2Q\cdot F)-Q^2(F^2q\cdot f+f^2q\cdot F)]+\frac{1}{M_W{}^4}[(F^2+f^2)F\cdot f+2F^2f^2][(Q^2+q^2)Q\cdot q-2q^2Q^2]\right\}. \tag{16}$$

The differential decay rate is

$$d\Gamma=\frac{1}{2m_Q}\tfrac{1}{2}\sum|\mathcal{M}|^2(2\pi)^{-5}\delta^4(Q-q-F-f)\prod_i\frac{d^3p_i}{2E_i}\,. \tag{17}$$

We define the following dimensionless quantities,

$$x=W^2/Q^2,\quad \omega=M_W{}^2/Q^2,\quad \gamma=\Gamma_W{}^2/Q^2,\quad \alpha=F^2/Q^2,\quad \beta=f^2/Q^2,\quad \delta=q^2/Q^2\,, \tag{18a}$$

and introduce a reference decay rate Γ_0

$$\Gamma_0=\frac{G^2m_Q{}^5}{192\pi^3}|U_{Qq}|^2\,. \tag{18b}$$

Integrating Eq. (17) first over the $F,\bar{f}$ phase space and then over q,W phase space, we obtain the differential decay rate

$$\frac{d\Gamma}{dx}=\Gamma_0\frac{\omega^2}{(x-\omega)^2+\omega\gamma}\lambda^{1/2}(1,\delta,x)\lambda^{1/2}(x,\alpha,\beta)$$
$$\times\left\{\frac{2}{x^2}\lambda(x,\alpha,\beta)(1+\delta-x)+\frac{2}{x^3}[x(x+\alpha+\beta)-2(\alpha-\beta)^2](1-\delta-x)(1+x-\delta)\right.$$
$$\left.+\frac{3}{x^2\omega^2}(x-2\omega)[(\alpha+\beta)x-(\alpha-\beta)^2][(1-\delta)^2-(1+\delta)x]\right\}. \quad (19a)$$

Here $\lambda(a,b,c)=a^2+b^2+c^2-2ab-2bc-2ca$. The limits on the variable x are

$$(\sqrt{\alpha}+\sqrt{\beta})^2\le x\le(1-\sqrt{\delta})^2 . \quad (19b)$$

The integration over x is carried out numerically. In the limiting case $\alpha=\beta=\gamma=0$, Eq. (19a) reproduces the result given in Ref. 19.

The decay width to a real W boson which subsequently decays to $F\bar{f}$ can be obtained from Eq. (19) by using the narrow-width limit

$$\frac{1}{(x-\omega)^2+\omega\gamma}\to\frac{\pi}{\sqrt{\omega\gamma}}\delta(x-\omega) . \quad (20)$$

Then analytic evaluation of the x integral gives the known result[19]

$$\Gamma=B(W\to F\bar{f})\frac{Gm_Q{}^3|U_{Qq}|^2}{8\pi\sqrt{2}}\lambda^{1/2}(1,\delta,\omega)$$
$$\times[\omega(1+\delta-\omega)+(1-\omega-\delta)(1+\omega-\delta)] . \quad (21)$$

For $\omega,\delta\ll1$, the partial width is given approximately by

$$\Gamma\simeq B(W\to F\bar{f})\frac{\alpha|U_{Qq}|^2}{16x_W}\frac{m_Q{}^3}{M_W{}^2} . \quad (22)$$

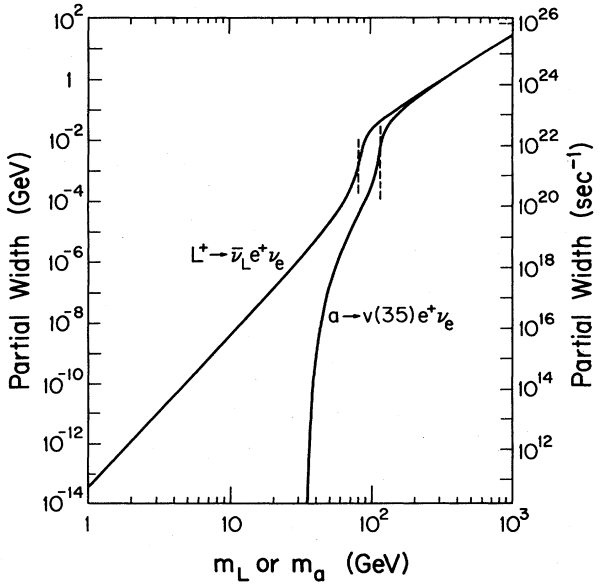

FIG. 1. Semileptonic partial decay widths of a heavy lepton L and a heavy $Q=\frac{2}{3}$ charge quark a, versus the mass of the decaying fermion. The dashed vertical lines denote thresholds for real-W emission.

Hence, for $m_Q\gg M_W$, we find the total width

$$\Gamma(Q\to qW)\simeq\frac{\alpha|U_{Qq}|^2}{16x_W}\frac{m_Q{}^3}{M_W{}^2}$$
$$\simeq(0.33\text{ TeV})|U_{Qq}|^2[m_Q/(1\text{ TeV})]^3 . \quad (23)$$

For $m_Q\lesssim400$ GeV, Γ_Q/m_Q is smaller than 5%, and we can safely neglect finite Q-width smearing in the decay distributions.

Figure 1 shows the partial width versus the mass of the decaying particle for the semileptonic transitions

$$L^+\to\bar{\nu}_L e^+\nu_e \text{ and } a\to v(35)e^+\nu_e$$

via a virtual or real W boson, calculated from Eq. (19) with $|U_{av}|\simeq1$. Note the cusps at the thresholds $m_L=M_W$ and $m_a=m_v+M_W$. The corresponding total widths can be estimated from these partial widths by multiplying by the number of contributing channels at the mass in question.

Figure 2 shows the calculated v-quark lifetime versus m_v, based on the mixing matrices of Eq. (11). For m_v comparable to or less than m_t (overlapping generations), the v lifetime may even be comparable to the τ, b, and c lifetimes, offering valuable opportunities for direct detection of v. In this circumstance vertex detectors at collider facilities could be vital in the study of v-quark physics.

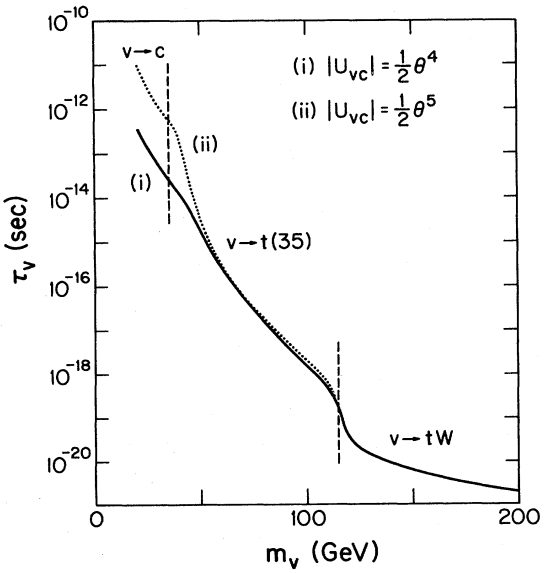

FIG. 2. Lifetime of a heavy $Q=-\frac{1}{3}$ charge quark v versus its mass calculated from the two choices of the mixing matrix in Eq. (11).

The possibility of a long-lived $Q=-\frac{1}{3}$ fourth-generation quark has also been noted by Pakvasa *et al.*[20]

All our considerations of weak decays are based on the standard electroweak model with one Higgs doublet. If in fact there exist further Higgs multiplets with a charged Higgs boson H light enough to be produced in heavy-quark decays,[21] then the $Q\to qH$ decay mode will dominate over virtual-W decay modes and may be comparable to the $Q\to qW$ decay rate.

III. PRODUCTION CROSS SECTIONS

In this section we present estimates of cross sections at hadron colliders for heavy-lepton production and for heavy (a or v) quark production, versus the particle mass. Specifically, cross sections are given for the CERN $p\bar{p}$ collider at $\sqrt{s}=0.54$ TeV, the Fermilab $p\bar{p}$ collider at $\sqrt{s}=2$ TeV, and a future pp or $p\bar{p}$ collider at center-of-mass energy $\sqrt{s}=20$ TeV. Some of our considerations overlap with those presented elsewhere.[22]

For calculations we consider two different sets of parton distributions:[23] (i) Owens-Reya (OR) with $\Lambda=0.3$ GeV, and (ii) Duke-Owens (DO) with $\Lambda=0.2$ GeV. These are evaluated at $Q^2=\hat{s}$, the energy squared of the parton subprocess. Unless otherwise specified the OR distributions are used. We assume an SU(3)-symmetric sea distribution throughout. The cross sections at $\sqrt{s}=20$ TeV are governed by the sea partons, since at this energy contributions from very low parton fractional momenta (typically $x\sim 0.01$) dominate. Consequently, the production cross sections at 20 TeV for heavy quarks of mass smaller than 300 GeV are nearly the same for pp and $p\bar{p}$. We remark that the extrapolations to 20 TeV depend on the validity of the Q^2 evolution of the parton sea of the QCD parametrization used.

For a collider that yields an annual luminosity of $\int dt\,\mathcal{L}=10^{37}\ \mathrm{cm}^{-2}$, a cross section of 10 pb corresponds to 100 events per year. We shall adopt this as a typical lower limit of feasibility for new quark and lepton searches. In searches based on lepton decay modes, the above signal will be reduced by the decay branching fractions by another factor of 5 to 10. Acceptance cuts will reduce the signal still further. For completeness, the production of fourth-generation charged leptons and neutrinos is also discussed briefly.

A. Heavy quarks

The lowest-order QCD subprocesses $q\bar{q},gg\to Q\bar{Q}$ are expected to provide a conservative lower estimate of heavy-quark hadroproduction. In evaluating these fusion contributions we used the usual form for the running coupling constant

$$\alpha_s(\hat{s})=12\pi/[(33-2n)\ln(\hat{s}/\Lambda_n^2)] \tag{24}$$

where n is the number of active flavors. The flavor number is increased by one at each threshold $(\hat{s})^{1/2}=2m_n$; the continuity of α_s is maintained by choice of the Λ_n. We choose $\Lambda_4=0.3$ GeV. Figure 3 gives the fusion cross sections versus the heavy-quark mass for both the OR and DO parton distributions. The predictions are similar at

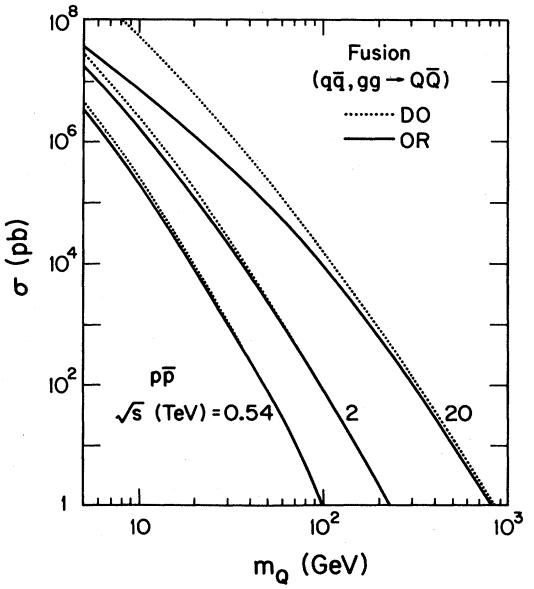

FIG. 3. QCD fusion ($q\bar{q},gg\to Q\bar{Q}$) cross sections for heavy-quark production based on two sets of parton distributions (Ref. 23).

0.54 and 2 TeV; the differences at 20 TeV are some measure of the uncertainty of the extrapolation.

In the case of charm, the fusion calculations underestimate the observed cross section at lower energies by a considerable factor.[24] The fusion graphs contribute only to central production while substantial forward production is observed. One proposed explanation[25] of the charm-production data ascribes the discrepancy to contributions of QCD flavor-excitation graphs.[26] The evaluation of these contributions depends on an assumed heavy-quark distribution in the nucleon and on a momentum-transfer

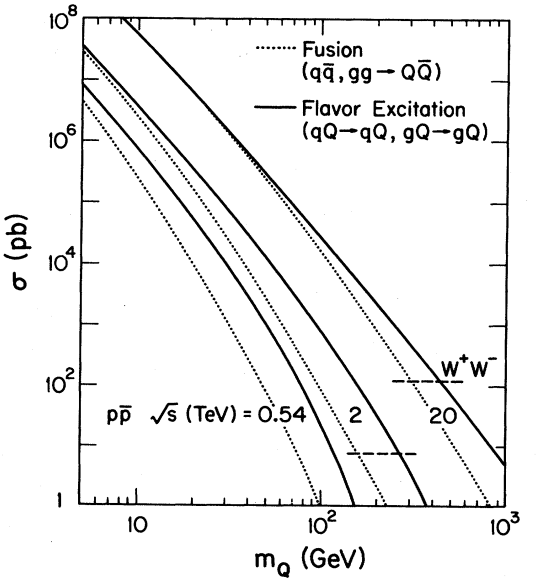

FIG. 4. Comparison of QCD flavor excitation ($gQ\to gQ, qQ\to qQ$) with fusion results using the DO parton distributions. The electroweak W^+W^- cross section is indicated by the dashed lines.

cutoff to obtain a finite result.[25,27] In Ref. 25 an extension of the flavor-excitation model to other heavy flavors was proposed. Following that extension, the results in Fig. 4 are obtained with the DO distributions. These flavor-excitation projections are intended only to illustrate that cross sections above that for fusion are an interesting possibility.

B. Heavy charged lepton

The primary source of heavy-charged-lepton production at hadron colliders is the decay $W \to L\bar{\nu}_L$. The feasibility of detecting a new heavy lepton of mass below 50 GeV from this source and differentiating its signal from backgrounds has already been extensively treated.[5] The most promising L signal is the large missing transverse momentum from $W \to L\bar{\nu}_L \to q'\bar{q}\nu_L\bar{\nu}_L$ and the hadronic jets from q' and $\bar{q}$. Our only extension of those results is to observe that the L signal from real or virtual W production is appreciable even when the L mass is comparable to or exceeds the W mass. Figure 5(a) shows the predicted L cross section versus its mass for both sets of parton distributions. Here it is assumed that the ν_L mass can be neglected.

Another source of heavy leptons, though smaller, is $L\bar{L}$ pair production via virtual photon and Z^0. These cross sections are shown in Fig. 5(b).

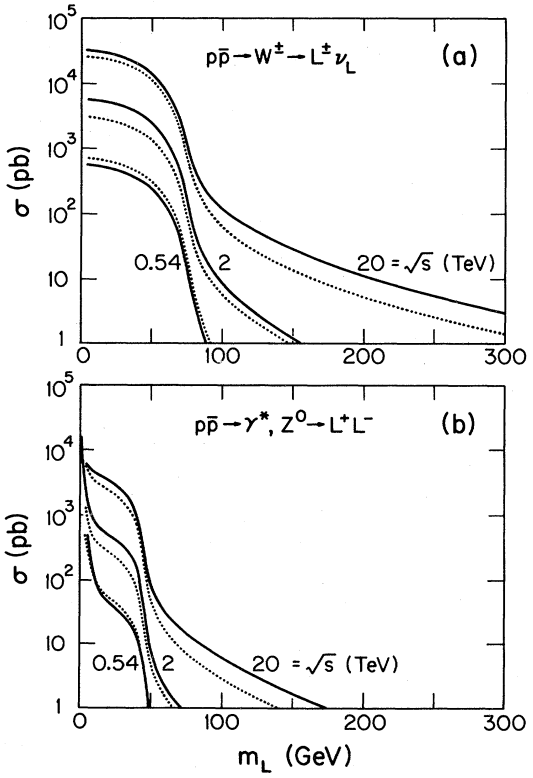

FIG. 5. Cross sections for heavy-lepton production via (a) $W \to L\nu_L$ and (b) $\gamma^*, Z \to L\bar{L}$ for two sets of parton distributions: OR (solid curves) and DO (dotted curves). A QCD-motivated factor $K = 2$ is included in the cross section.

C. Sequential neutrino

The primary sources of fourth-generation neutrino production at hadron colliders are the decay $W \to L\bar{\nu}_L$ treated above the decay $Z \to \nu_4\bar{\nu}_4$. The latter gives a $\nu_4\bar{\nu}_4$ rate much larger than the $L\bar{L}$ rate shown in Fig. 5(b). We assume that the charged-current neutral eigenstate ν_L is mainly composed of the fourth neutrino mass eigenstate ν_4 with mass much less than the charged-lepton mass. The most promising signal for ν_4 is its charged-current decay in flight $\nu_4 \to lq\bar{q}'$, $l\nu\bar{l}'$, where $l = e,\mu,\tau$ as discussed by Barger, Keung, and Phillips.[6]

If ν_4 is a Majorana particle, there is a correction to the $Z \to \nu_4\nu_4$ partial width and more importantly to ν_4 decay since both lepton signs are now accessible: $\nu_4 \to l^{\pm}X$. This allows same-sign dilepton events $Z \to \nu_4\nu_4 \to l^+l^+XX'$ that would be forbidden for Dirac neutrinos (see Ref. 6).

IV. DISTRIBUTIONS OF DECAY PARTICLES

Experimental searches for heavy-quark decay fragments will likely concentrate on leptons emitted in semileptonic decays in order to avoid hadronic QCD backgrounds. In this section we detail some typical expectations for the decay distributions of superheavy quarks and compare the decay spectra with those from a t quark of mass 35 GeV. The shapes of the distributions are of primary interest. For normalizations we take the QCD fusion results for $Q\bar{Q}$ production and use semileptonic branching fractions of 0.1 when the decays proceed via virtual W and 0.08 when the decay into real W is kinematically accessible, the difference being the assumed importance of the $t\bar{b}$ channel. We concentrate on the case of Q decaying semileptonically and $\bar{Q}$ decaying hadronically (observed rates summed over both charged leptons will be a factor of 2 higher than the rates shown in the figures). The heavy-quark decays are represented by spin averages of the usual $V-A$ matrix elements squared in Eq. (16). Only the primary $Q \to qe\nu$ decay stages are taken into account since the high-transverse-momentum "trigger" charged leptons are dominantly of this origin.[4] Secondary neutrinos emitted in cascade stages of the decay will smear the distributions involving missing transverse momentum somewhat,[1,4] but the essential features should persist.

Comparisons will be made among the following possible sources:

$$
\begin{aligned}
&\text{(S1)}\quad t(35) \to be\nu\,, \\
&\text{(S2)}\quad v(35) \to ce\nu\,, \\
&\text{(S3)}\quad v(50) \to t(35)e\nu\,, \\
&\text{(S4)}\quad v(90) \to t(35)e\nu\,, \\
&\text{(S5)}\quad a(150) \to v(90)e\nu\,, \\
&\text{(S6)}\quad v(150) \to t(35)W^-\,, \\
&\text{(S7)}\quad a(150) \to v(35)W^+\,, \\
&\text{(S8)}\quad W^+W^- \text{ (electroweak)}\,.
\end{aligned}
\tag{25}
$$

Here the numbers in parentheses denote the assumed heavy-quark mass. The problem of disentangling overlapping quark generations is addressed in Sec. V. Of the above decay modes, real-W emission is possible only in (S6) and (S7). The W^+W^- electroweak production calculation is described in Sec. VI. We mostly consider distributions in transverse variables since these are insensitive to the parton distributions.

A. Electron transverse momentum

Figure 6 shows the distributions from a number of the above sources at $\sqrt{s}=2$ and 20 TeV of the electron momentum p_{eT} transverse to the beam axis. As M_Q increases, the p_{eT} distribution becomes flatter. However, the t-quark contribution (and also the b,c contributions[1,4]) constitutes a severe background. Consequently, some lepton isolation criteria must be invoked to separate out the a,v signals, analogous to that advocated in Ref. 4 for separating the t signal from the b,c backgrounds.

For a heavy-quark decay the average of the momenta transverse to the jet axis is[4]

$$\left\langle \sum_i |\vec{p}_{i\perp}| \right\rangle = \pi m_Q/4 \ . \tag{26}$$

The scale of the decay transverse momenta is set by m_Q. Hence, heavy a and v jets will be typically fatter and have decay electrons with larger $p_\perp$ transverse to the jet axis, than t jets.

B. Momentum of $e\nu$ normal to Q production plane

In the decay $Q\to qe\nu$ the component of the $e\nu$ momentum along the normal to the production plane

$$\vec{N}=\vec{p}_Q\times\vec{p}_{\text{beam}}=\vec{p}_{QT}\times\vec{p}_{\text{beam}} \tag{27}$$

has a distribution whose end point

$$(p_{e\nu})_N=\frac{m_Q{}^2-m_q{}^2}{2m_Q} \tag{28}$$

is determined by the quark masses. Figure 7 shows $(p_{e\nu})_N$ distributions of several heavy-quark sources. In the $v(150)\to t(35)$ case, the distribution is flat out to the value

$$(p_{e\nu})_N=\tfrac{1}{2}m_Q\lambda^{1/2}(1,m_q{}^2/m_Q{}^2,M_W{}^2/m_Q{}^2) \tag{29}$$

which is the kinematic end point for real-W emission. The region between Eq. (29) and the end point of Eq. (28) corresponds to a virtual W that decays to $e\nu$. Provided that the missing transverse momentum is measured with sufficient accuracy, so that resolution smearing of b,c,t contributions does not obscure the high-$(p_{e\nu})_N$ region, this distinctive p_N distribution may be useful in heavy-quark searches.

C. Transverse masses

The initial light quarks or gluons can acquire transverse momentum from gluon emission which will smear somewhat the transverse-momentum distributions of Figs. 6 and 7. Although this smearing can be included by explicit calculation,[4,28] it is advantageous to work instead with quantities like transverse mass that are insensitive to transverse boosts.[29] The transverse mass of the electron plus its associated neutrino in $Q\to qe\nu$ decay is defined by

$$M_T{}^2(e,\nu)=(|\vec{p}_{eT}|+|\vec{p}_{\nu T}|)^2-|\vec{p}_{eT}+\vec{p}_{\nu T}|^2 \tag{30}$$

and obeys the bounds[1]

$$0\le M_T(e,\nu)\le m_Q-m_q \ . \tag{31}$$

Figure 8 shows typical $M_T(e,\nu)$ distributions. For heavy

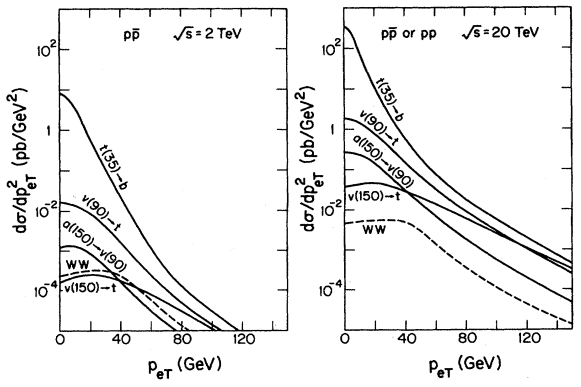

FIG. 6. Electron momentum distribution transverse to the beam axis resulting from the decay $Q\to qe\nu$.

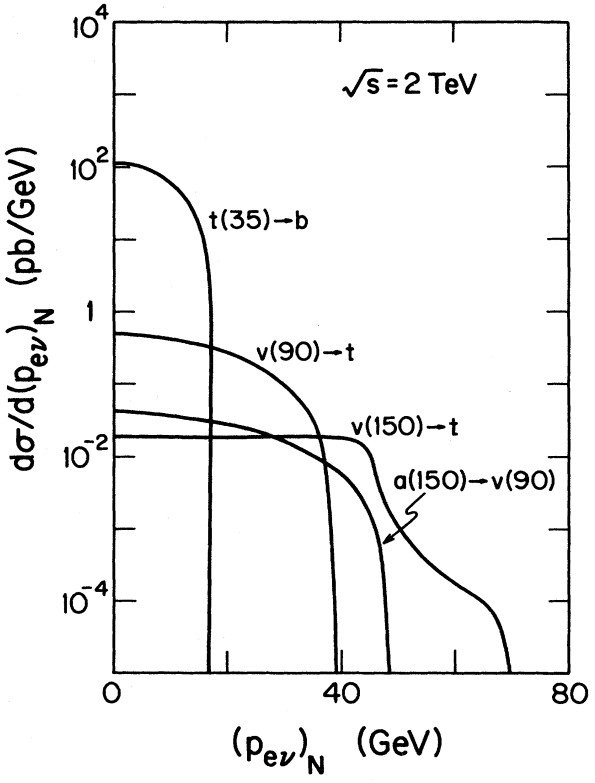

FIG. 7. The $e\nu$ momentum distribution along the normal to the production plane $\vec{N}=\vec{p}_{QT}\times\vec{p}_{\text{beam}}$ from the decay $Q\to qe\nu$. The normalization corresponds to the fusion cross section at a 2-TeV $p\bar{p}$ collider; relative comparisons of the distributions at 20 TeV are very similar. The distribution for $a(150)\to v(35)+W^+$ decay is the same as $V(150)\to t(35)+W^-$.

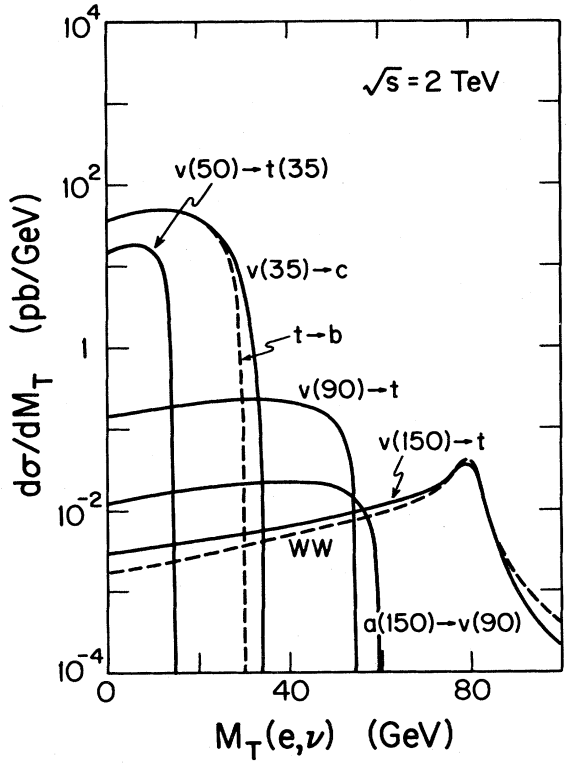

FIG. 8. Transverse-$e\nu$-mass distribution $M_T(e,\nu)$ from $Q\to qe\nu$ decays. Similar results are obtained at 20 TeV, except for overall normalization.

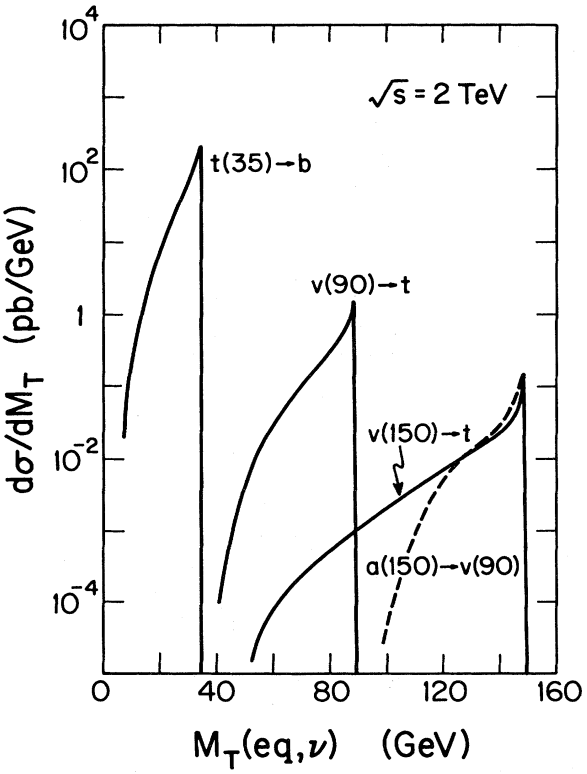

FIG. 9. Cluster-transverse-mass distribution $M_T(qe,\nu)$ from $Q\to qe\nu$ decays.

quarks that decay to a real W, a Jacobian peak appears near $M_T=M_W$. The $Q\bar{Q}$ events with real-W decays are distinguished from the electroweak single W and W pair production by the hadronic activity associated with q jets.

If the recoil q jet is identified, it can be included in various ways; the optimum variable[1] is the "cluster" transverse mass $M_T(qe,\nu)$ defined by

$$M_T^2(qe,\nu)=[(|\vec{p}_{qeT}|^2+m_{qe}^2)^{1/2}+|\vec{p}_{\nu T}|]^2 -(\vec{p}_{qeT}+\vec{p}_{\nu T})^2 \quad (32)$$

that incorporates the recoil-q-jet information and has a sharp Jacobian peak at its endpoint m_Q. Here p_{qe} and m_{qe} denote the momentum and invariant mass of the q-jet plus electron system, regarded as a single entity. Figure 9 shows typical distributions in this variable. Resolution smearing will give tails to these Jacobian peaks above m_Q, but the actual distributions will still be peaked at the Q mass (see Ref. 4 and Sec. V for examples).

D. Topological signatures

Identification of heavy quarks produced at colliders may be possible through the topological properties of the events. For example, such criteria have been proposed[1,4,5] to separate $c\bar{c}$, $c\bar{s}$, $b\bar{b}$, $t\bar{b}$, and $t\bar{t}$ events on the basis of jet broadness: the c,b quarks lead to highly collimated jets which are distinguishable from the broad distributions of particles expected from the t quark. The essential point has been made in Eq. (26) above; such ideas have been successfully exploited to tag heavy flavor in e^+e^- events at DESY PETRA.[30] If the jet p_T enormously exceeds the quark mass, jet broadening is determined by QCD radiation rather than m_Q, but this is not the regime that we are considering here. Furthermore, microvertex detectors should be able to distinguish the one-step and two-step topologies of c and b decays. In addition, the $W\to t\bar{b}$ process gives a characteristic Jacobian peak in the $\bar{b}$ transverse momentum, which should allow these events to be separated from $t\bar{t}$ events. Similar ideas can be exploited in identifying fourth-generation quarks; we discuss some examples in the following.

(i) First, suppose $m_\nu\approx m_t$ and $m_a\gg m_\nu$. Then $a\bar{a}$ and $a\bar{\nu}$ production are suppressed relative to $\nu\bar{\nu}$ and $t\bar{t}$, while the latter have superficially similar decays $\nu\to c$, $t\to b$. Vertex detectors, however, should allow the c and b jets to be distinguished. Furthermore, the t-mass can be separately determined from the $W\to t\bar{b}$ process. See Sec. V for further discussion.

(ii) Suppose $m_t<m_\nu<M_W<m_a$: Then $\nu\bar{\nu}$ production is the principal fourth-generation-quark effect, somewhat suppressed relative to $t\bar{t}$. However, $\nu\bar{\nu}$ production with semileptonic $\nu\to te\nu$ decay should be distinguishable from $t\bar{t}$ production with $t\to be\nu$ decay, by the greatly differing broadness of the secondary quark jet (t,b, respectively) and of the associated spectator jet ($\bar{\nu},\bar{t}$, respectively). The mean multiplicity of decay particles should also be higher for $\nu\bar{\nu}$ than for $t\bar{t}$ events.

(iii) Suppose $M_W+m_t<m_\nu<m_A$; in this case $\nu\bar{\nu}$ pairs decay to $W^+W^-t\bar{t}$. The presence of $W^\pm$ is signalled by the Jacobian peak of $M_T(e,\nu)$ shown in Fig. 8, while the second W leads to two quark jets 75% of the time. The

$v\bar{v}$ contribution is distinguishable from single W and W^+W^- electroproduction by the associated hadronic activity.

(iv) Finally, consider $a\bar{a}$ production. The primary decay is likely $a \to v$, provided that $m_v < m_a$, and then v decays according to one of the above schemes. The final state will have high multiplicity and multiple jets, where detailed properties can be better spelled out when m_v and the v-decay modes are known. However, in the event that $m_b + M_W < m_a < m_v + M_W$, the decay mode $a \to bW$ could contribute.

The production of fourth-generation quarks will also greatly enlarge the range of possible multilepton configurations that result from the semileptonic branches of cascade decays.

V. THE CASE OF OVERLAPPING QUARK GENERATIONS: HOW TO DISTINGUISH v AND t SIGNALS

The possibility that there may exist a charge $-\frac{1}{3}$ v quark with mass less than t has been largely overlooked. Should this be the case, previous expectations for heavy-quark signals from t alone would require radical revision.

Hadroproduction of heavy quarks is flavor blind and falls steeply as the mass of the produced quarks increases.

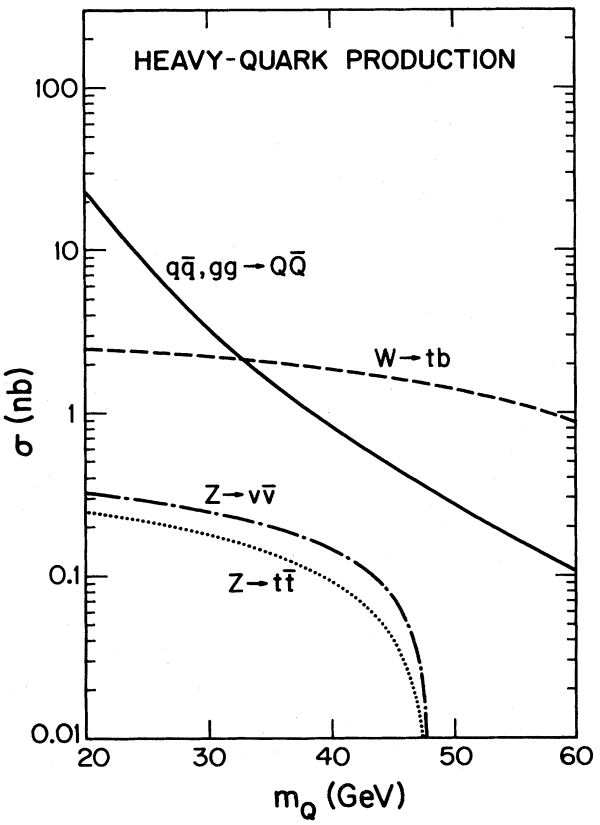

FIG. 10. Cross sections for heavy-quark $Q = v,t$ production versus mass m_Q at $\sqrt{s} = 620$ GeV, comparing different channels (i) $q\bar{q},gg \to Q\bar{Q}$ hadroproduction (solid curve), (ii) $q\bar{q} \to W^{\pm} \to t\bar{b},b\bar{t}$ electroweak production (dashed curve), (iii) $q\bar{q} \to Z^0 \to v\bar{v}$ production (dash-dotted curve), (iv) $q\bar{q} \to Z^0 \to t\bar{t}$ production (dotted curve).

Hence for overlapping generations the hadroproduction cross section for $v\bar{v}$ pairs is necessarily greater than that for $t\bar{t}$ pairs. Since the semileptonic branching fractions for $v \to cl\bar{\nu}$ and $t \to b\bar{l}\nu$ are expected to be similar (by counting final state fermion channels), the number of primary decay leptons from $v\bar{v}$ exceeds those from $t\bar{t}$ decays.

Electroweak production differs between v and t quarks. The channel $p\bar{p} \to W^{\pm}X$, $W^{\pm} \to t\bar{b},b\bar{t}$ is unlikely to have a v-production counterpart because $W \to a\bar{v}$ is probably forbidden kinematically and $W \to c\bar{v},t\bar{v}$ are expected to be strongly suppressed by weak mixing angles. The channel $p\bar{p} \to Z^0X$, $Z \to v\bar{v}$ is somewhat preferred over $Z \to t\bar{t}$, but both give much smaller rates than the $W \to t\bar{b}$ process.

Figure 10 compares the v- and t-quark cross sections from these different sources as functions of the quark mass at $\sqrt{s} = 620$ GeV, corresponding to the 1984 energy of the CERN collider. We use the OR parton distributions[23] and fusion processes only with the QCD-motivated enhancement factors $K = 2$ for both strong and electroweak production; this agrees with the observed W and Z production rates.[3] Possible contributions from flavor excitation[25,27] are ignored.

A promising trigger for heavy quarks is a single lepton with high momentum p_T transverse to the beam axis, from semileptonic decay.[1,2] A minimum p_T cut is necessary for lepton identification. In this context the v-quark signals are very similar to (and stronger than) those from t quarks. Figure 11 shows the single-lepton cross sections from the various v- and t-quark sources versus the p_T cut

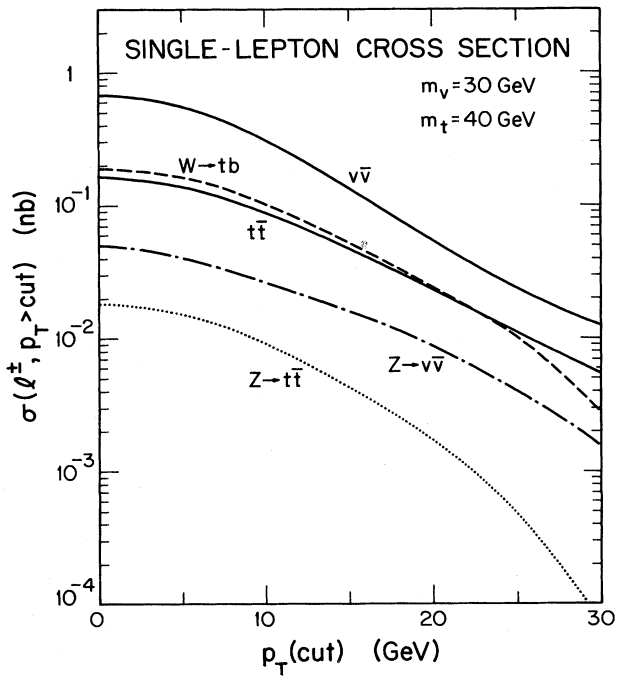

FIG. 11. Cross sections for primary leptons from decays of v and t quarks at $\sqrt{s} = 620$ GeV, versus lepton p_T cut, assuming $m_v = 30$ GeV and $m_t = 40$ GeV; (i) hadroproduction (solid curves), (ii) $W \to t\bar{b},b\bar{t}$, (dashed curve), (iii) $Z^0 \to v\bar{v}$ (dashed dotted curve), and (iv) $Z^0 \to t\bar{t}$ (dotted curve). The cross section shown is summed over both signs for a given lepton: $\sigma \equiv \sigma(\mu^+) + \sigma(\mu^-) = \sigma(e^+) + \sigma(e^-)$.

at $\sqrt{s}=620$ GeV, for $m_v=30$ GeV and $m_t=40$ GeV. This figure shows that the net single-lepton cross section from heavy quarks is dominated by the postulated v-quark signals (assuming that b- and c-quark backgrounds can be removed by lepton isolation criteria [4]).

Primary leptons from $W\to t\bar{b}$, $t\to b\bar{l}\nu$ decays have distinctive signatures;[1] in particular, the fast narrow recoil b jet with its Jacobian peak in p_T distinguishes this process from $t\bar{t}$ and $v\bar{v}$ events with broad recoil $\bar{t}$ and $\bar{v}$ jets. Thus, W-initiated events should be sufficient by themselves to establish the existence of t and to determine its mass.

The hadroproduced $v\bar{v}$ and $t\bar{t}$ events may be hard to distinguish event-by-event. However, if the v and t masses are not degenerate, a single-quark mass will not suffice to describe the observed distributions. It may be possible to separate two distinct mass peaks by a judicious choice of distribution such as the cluster mass, defined by Eq. (32) and shown in Fig. 12. The calculations here include smearing effects on missing p_T arising from extra neutrinos in the $t\to b\to c\to s$ cascade decays and also from measurement errors represented by a Gaussian distribution with 4-GeV standard deviation in each transverse coordinate. Uncertainties from q-jet reconstruction are not known but should in practice be added. Figure 12 shows that although the $v\bar{v}$ and $t\bar{t}$ single-charged-lepton signals are rather similar, it may be possible to distinguish the presence of two distinct peaks in the cluster transverse mass distribution. Failing this, a comparison of mass

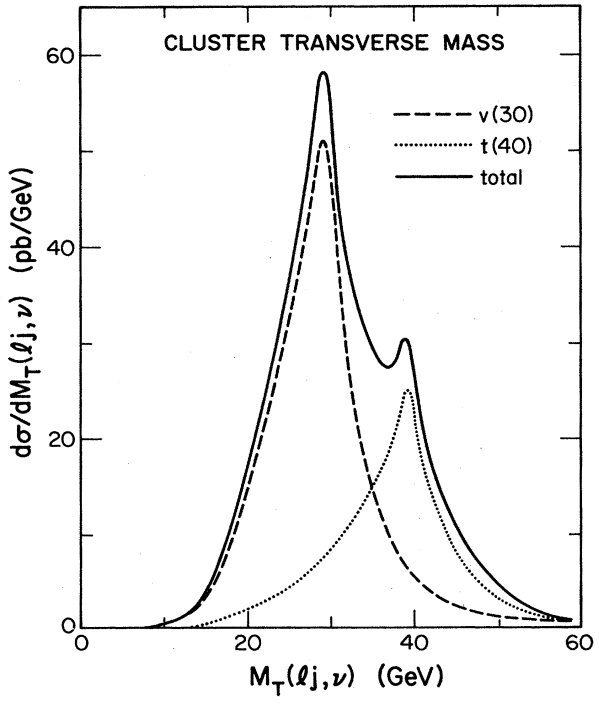

FIG. 12. Cross section versus cluster transverse mass at $\sqrt{s}=620$ GeV for $m_v=30$ GeV, $m_t=40$ GeV, distinguishing different contributions: (i) $v\bar{v}$ events (dashed curve), (ii) $t\bar{t},t\bar{b},b\bar{t}$ events (dotted curve), and (iii) total (solid curve). The lepton is required to have $p_T>5$ GeV. Realistic smearing of missing neutrino momentum is included.

determinations from $W\to t\bar{b}$ and from $v\bar{v},t\bar{t}$ hadroproduction events should show a discrepancy and allow the v mass to be estimated.

There are supplementary ways to discriminate between v and t events, exploiting their different lifetimes and decay products. If v has a lifetime of 10^{-13} sec or longer (see Fig. 2), microvertex detectors may be able to distinguish the spatial separation between the initial production and decay vertices in some fraction of events.

In candidate v or t events, the identification of b- or c-flavored hadrons among the decay products should be feasible sometimes either from kinematic reconstruction or from vertex detection. This could in turn choose between v and t interpretations; e.g., presence of a b-hadron would exclude a $v\bar{v}$ interpretation, while evidence for a primary $Q\to c$ decay would indicate $Q=v$. Without identifying specific heavy hadrons, there is still a possibility to distinguish some b jets from c jets by the distribution in p_T relative to the jet axis following Eq. (26) and Sec. IV D.

Furthermore, the multilepton final states, arising from the semileptonic branches of the heavy-quark cascade decay chains, are different in $v\bar{v}$ and $t\bar{t},t\bar{b}$ events. For example, like-sign trileptons $l_1^+l_2^+l_3^+$ or $l_1^-l_2^-l_3^-$ cannot arise from $v\bar{v}$. The cross sections are very small, however.[31]

Finally, if diffractive or flavor-excitation production of heavy $Q\bar{Q}=v\bar{v},t\bar{t}$ is important, the contributions at large positive longitudinal momentum fraction x (defined here relative to the *proton* momentum) should be dominated by baryons $\Lambda_Q(Qud)$, $\Sigma_Q(Quu,Qud)$ and mesons $M_Q(\bar{Q}u,\bar{Q}d)$. At large negative x the corresponding antiparticles dominate. By counting rule arguments[32] the cross sections scale in the limit $|x|\to 1$ according to

$$\sigma(\Lambda,\Sigma)\sim(1-|x|)\,,\qquad \sigma(M)\sim(1-|x|)^3\,. \tag{33}$$

This behavior is compatible with the accelerator data on diffractive charm production.[24] The charge of the lepton in the primary semileptonic decay of a given baryon or meson differs between $Q=v$ and t alternatives, and could thereby distinguish these sources if the type of parent particle is known (e.g., as $x\to 1$ baryons dominate and leptons l^+,l^- indicate the flavor t,v respectively.)

Figure 13 illustrates how the x_l distributions of primary decay leptons (with $p_T>5$ GeV) from diffractively produced t- or v-flavored hadrons may differ at $\sqrt{s}=620$ GeV, specializing to the forward hemisphere $x>0$, in the proton direction. We assume masses $m_v=30$ GeV, $M_t=40$ GeV, and longitudinal-hadron-momentum distributions

$$\frac{d\sigma}{d|x|}\sim(1-|x|)^n \tag{34}$$

with $n=1,3$, corresponding to the baryon and meson cases, respectively. The total diffractive cross sections are assumed to be proportional to $(m_Q)^{-2}$, as is the case in some models.[24,32] For illustration the ratio of mesonic to baryonic production is taken to be one, but this is not necessarily the case. The diffractive-model results in Fig. 13 show that if the generations overlap, then v-

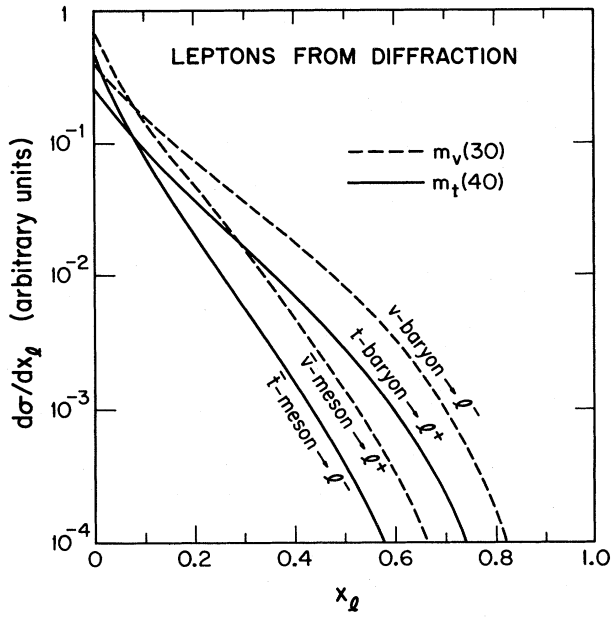

FIG. 13. Distributions of primary ν- and t-decay leptons in the forward (proton direction) hemisphere versus longitudinal-momentum fraction x_l at $\sqrt{s}=620$ GeV, assuming diffractive distributions of the parent hadrons $d\sigma/dx \sim (1-x)^n$ with $n=1$ for baryons and $n=3$ for mesons, and a total diffractive cross section that scales like $(m_Q)^{-2}$. Masses $m_\nu=30$ GeV and $m_t=40$ GeV are assumed. The lepton is required to have $p_T>5$ GeV.

baryon $\to l^-$ should indeed dominate at large positive m_l, whereas otherwise t-baryon $\to l^+$ should dominate here.

The foregoing considerations presuppose that lepton backgrounds from b and c decays (including secondary contributions from $\nu\to c$ and $t\to b$ cascades) can be suppressed by suitable isolation cuts[4] and that the electromagnetic Drell-Yan background can be suppressed by requiring substantial hadronic activity as expected in the heavy-quark events.

VI. ELECTROWEAK W-PAIR PRODUCTION

Superheavy quarks that decay via $Q\to qW$ give final states with W pairs plus q and $\bar{q}$ decay jets. This topology should be readily distinguished from electroweak W^+W^- pair production[33–35] in which the accompanying hadronic activity should be primarily longitudinal. Backgrounds from the higher-order QCD W^+W^- process with the emission of hard gluons are expected to be significantly suppressed relative to the lowest-order electroweak contribution.

The electroweak W-pair production process is very interesting in its own right as a test of electroweak gauge theory. In addition, its cross section and distributions could serve as a useful benchmark with which superheavy-quark contributions could be compared.

In this section we give formulas for the differential cross section for W^+W^- production with W^- decay to $e^-\bar{\nu}_e$. Full polarization correlations involving the virtual W^- state are taken into account; a different approach to this calculation is given in Ref. 35, based on density matrices.

Figure 14 shows the relevant quark subprocesses, whose amplitudes we mnemonically label as u, d, γ, and Z, respectively. With momenta labels as in Fig. 14, the amplitudes are given by

$$\begin{aligned}
\mathcal{M}_u &= (\hat{u})^{-1} R_{\lambda\nu}\bar{v}(\bar{q})\gamma_\nu(2q_\lambda+\gamma_\lambda \not{W})(1-\gamma_5)u(q)\ ,\\
\mathcal{M}_d &= -(\hat{t})^{-1} R_{\lambda\nu}\bar{v}(\bar{q})(2\bar{q}_\lambda+\not{W}\gamma_\lambda)\gamma_\nu(1-\gamma_5)u(q)\ ,\\
\mathcal{M}_\gamma &= 8x_W Q_q(\hat{s})^{-1} R_{\lambda\nu}\bar{v}(\bar{q})(\not{W}g_{\nu\lambda}+k_\lambda\gamma_\nu-W_\nu\gamma_\lambda)u(q)\ ,\\
\mathcal{M}_Z &= 4(\hat{s}-M_Z{}^2+iM_Z\Gamma_Z)^{-1} R_{\lambda\nu}\\
&\quad\times\bar{v}(\bar{q})(\not{W}g_{\nu\lambda}+k_\lambda\gamma_\nu-W_\nu\gamma_\lambda)(a_Z-b_Z\gamma_5)u(q)\ ,
\end{aligned} \tag{35}$$

where $\hat{u}=(q-W)^2$, $\hat{t}=(\bar{q}-W)^2$, $x_W=\sin^2\theta_W$, and

$$\begin{aligned}
R_{\lambda\nu} &= e^3\epsilon_\lambda(W)(8\sqrt{2}\sin^3\theta_W)^{-1}(k^2-M_W{}^2+iM_W\Gamma_W)^{-1}\\
&\quad\times\bar{u}(l)\gamma_\nu(1-\gamma_5)v(\bar{\nu})\ .
\end{aligned} \tag{36}$$

The electroweak quark couplings that appear in $\mathcal{M}_Z$ are

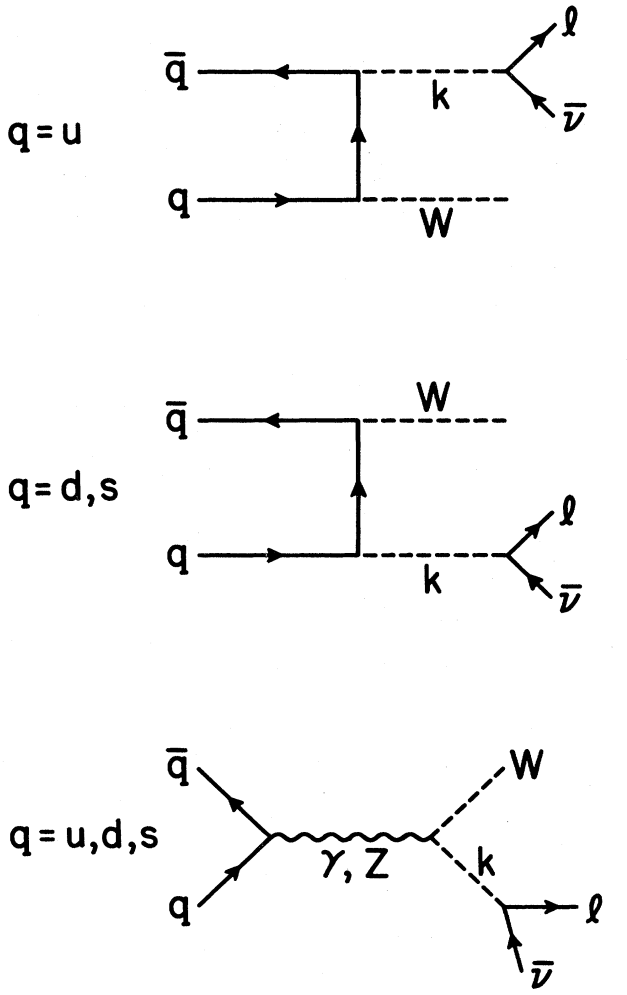

FIG. 14. Momentum labels of quark subprocesses for electroweak W^+W^- production; k, l, and $\bar{\nu}$ denote the W^-, electron, and antineutrino outgoing momenta, respectively.

$$a_Z = T_3 - 2Q_q x_W \ , \qquad b_Z = T_3 \ , \tag{37}$$

where Q_q is the electric charge and T_3 the third component of weak isospin of the incident parton. The square of $\mathcal{M}$, summed over spins and colors, is evaluated using the computer algebraic program ASHMEDAI and checked by hand. The result including all parton subprocesses is of the form

$$\sum |\mathcal{M}|^2 = \frac{3e^6}{(k^2-M_W{}^2)^2+M_W{}^2\Gamma_W{}^2} \times \left[E_q + I_q + \sum_{V,V'=\gamma,Z} S_{VV'}\right] . \tag{38}$$

Here E_q represents the square of a quark-exchange diagram,

$$E_u = \frac{2}{x_W{}^3 \hat{u}^2}[2(M_W{}^2-\hat{u})W\cdot\bar{\nu}\bar{q}\cdot l - (2M_W{}^2-\hat{u}^2/M_W{}^2)q\cdot\bar{\nu}\,\bar{q}\cdot l] \ , \tag{39}$$

$$E_d = E_u(q\leftrightarrow\bar{q},\ l\leftrightarrow\bar{\nu}) \ .$$

The I terms are interferences of the quark-exchange diagrams with direct-channel γ,Z diagrams

$$I_u = \left\{\frac{8Q_u}{\hat{s}\,\hat{u}x_W{}^2} + \frac{4(a_Z+b_Z)(\hat{s}-M_Z{}^2)}{[(\hat{s}-M_Z{}^2)^2+M_Z{}^2\Gamma_Z{}^2]\hat{u}x_W{}^3}\right\}F \ , \tag{40}$$

$$I_d = I_u(q\leftrightarrow\bar{q}, l\leftrightarrow\bar{\nu}, Q_u\leftrightarrow Q_d) \ .$$

Here the quantity F is given by

$$F = -q\cdot\bar{\nu}\,\bar{q}\cdot l[\hat{s}+M_W{}^2+k^2+\hat{u}(\hat{s}-k^2)/M_W{}^2]+q\cdot\bar{\nu}\,q\cdot l(\hat{t}-M_W{}^2)+\bar{q}\cdot l\,\bar{\nu}\cdot W(\hat{s}-\hat{u}+M_W{}^2) + \tfrac{1}{2}\bar{q}\cdot l\,k^2(\hat{u}-M_W{}^2)+W\cdot l\,q\cdot\bar{\nu}\hat{s}+\bar{q}\cdot\bar{\nu}\,q\cdot l M_W{}^2-M_W{}^2k^2\hat{s}/4 \ . \tag{41}$$

Finally, the $S_{VV'}$ terms are the squares and interference of the direct-channel diagram. These can be expressed in the form

$$S_{VV'} = 16C_{VV'}[(a_Va_{V'}+b_Vb_{V'})G_1+(a_Vb_{V'}+b_Va_{V'})G_2] \ , \tag{42}$$

where $a_\gamma=1$, $b_\gamma=0$, a_Z, and b_Z appeared in Eq. (37),

$$C_{\gamma\gamma} = \frac{Q_q{}^2}{2x_w\hat{s}^2}, \quad C_{\gamma Z} = C_{Z\gamma} = \frac{Q_q(\hat{s}-M_Z{}^2)}{4x_W{}^2\hat{s}[(\hat{s}-M_Z{}^2)^2+M_Z{}^2\Gamma_Z{}^2]} \ , \quad C_{ZZ} = \frac{1}{8x_W{}^3[(\hat{s}-M_Z{}^2)^2+M_Z{}^2\Gamma_Z{}^2]} \ . \tag{43}$$

The invariant quantities G_1 and G_2 are

$$G_1 = [\bar{q}\cdot\bar{\nu}\,q\cdot l+q\cdot\bar{\nu}\,\bar{q}\cdot l][M_W{}^2-2k^2-2\hat{s}+(\hat{s}-k^2)^2/M_W{}^2] + 2[q\cdot l\,W\cdot\bar{\nu}+q\cdot\bar{\nu}\,W\cdot l+\bar{q}\cdot l\,W\cdot l+\bar{q}\cdot l\,W\cdot\bar{\nu}]\hat{s}-\tfrac{1}{2}[(k^2-\hat{t})(M_W{}^2-\hat{t})+(K^2-\hat{u})(M_W{}^2-\hat{u})]k^2-M_W{}^2k^2\hat{s} \ , \tag{44a}$$

$$G_2 = [\bar{q}\cdot\bar{\nu}\,q\cdot l-q\cdot\bar{\nu}\,\bar{q}\cdot l][3M_W{}^2+2k^2+2\hat{s}-(\hat{s}-k^2)^2/M_W{}^2] + [q\cdot(\bar{\nu}-l)(\hat{t}-M_W{}^2)+\bar{q}\cdot(l-\bar{\nu})(\hat{u}-M_W{}^2)]k^2+2[\bar{q}\cdot l\,W\cdot\bar{\nu}+q\cdot l\,W\cdot l-\bar{q}\cdot\bar{\nu}\,W\cdot l-q\cdot l\,W\cdot\bar{\nu}]\hat{s} \ . \tag{44b}$$

The differential cross section for a quark subprocess is

$$d\hat{\sigma} = \frac{1}{2\hat{s}}\frac{1}{4}\frac{1}{9}\sum|\mathcal{M}|^2(2\pi)^{-5}\delta^4(q+\bar{q}-l-\bar{\nu}-W)\prod_i\frac{d^3p_i}{2E_i} \ . \tag{45}$$

The differential cross section for $p\bar{p}$ production is

$$\frac{d\sigma}{dx_1dx_2} = \sum_{q=u,d,s}[f_{q/p}(x_1,Q^2)f_{\bar{q}/\bar{p}}(x_2,Q^2)d\hat{\sigma}(q\bar{q})+f_{\bar{q}/p}(x_1,Q^2)f_{q/\bar{p}}(x_2,Q^2)d\hat{\sigma}(\bar{q}q)] \ , \tag{46}$$

where x_1 and x_2 are the fractional momenta of the partons. Also, $f_{a/b}$ is the probability distribution of quark a in hadron b, which is QCD evolved up to $Q^2=\hat{s}$; $d\hat{\sigma}(\bar{q}q)$ is obtained from $d\hat{\sigma}(q\bar{q})$ by interchanging the q and $\bar{q}$ three momentum directions. The W^+W^- cross sections and distributions shown in preceding figures were based on these formulas, which reproduce the cross-section results of Ref. 33 for real-WW production.

VII. SUMMARY

In this paper we have attempted to identify salient features of the production and decay of fourth-generation quarks and leptons at pp and $p\bar{p}$ colliders. For quarks we have introduced plausible extensions of the weak-current mixing matrix that have increasing suppression of cross-generational transitions. With overlapping generations ($m_\nu \sim m_t$), we find particularly interesting physics results,

such as a long υ lifetime and a confusion of υ and t signals. Another interesting possibility is the existence of superheavy quarks that decay to a real W boson. We have given representative transverse distributions of heavy-quark decay fragments and discussed topological event properties that could be useful in the experimental identification of signals from fourth-generation quarks. We have discussed in particular detail the problems of disentangling υ- and t-quark signals should their masses overlap.

A summary of most of the above results was presented[36] at the Physics of the 21st Century Conference at Tuscon, Arizona in 1983.

ACKNOWLEDGMENTS

We thank F. Halzen for discussions on flavor excitation, T. Weiler for a helpful reference, and J. Ohnemus for checking some calculations. This research was supported in part by the University of Wisconsin Research Committee with funds granted by the Wisconsin Alumni Research Foundation, and in part by the Department of Energy under Contract No. DE-AC02-76ER00881.

[1]V. Barger, A. D. Martin, and R. J. N. Phillips, Phys. Lett **125B**, 339, 343 (1983); Phys. Rev. D **28**, 145 (1983).

[2]R. M. Godbole, S. Pakvasa, and D. P. Roy, Phys. Rev. Lett. **50**, 1539 (1983); G. Ballocchi and R. Odorico, Phys. Lett. **136B**, 126 (1984); F. Halzen, and D. M. Scott, Phys. Lett. **129B**, 341 (1983); L. M. Sehgal and P. Zerwas, Nucl. Phys. **B234**, 61 (1984); K. Hagiwara and W. F. Long, Phys. Lett. **132B**, 202 (1983); R. Horgan and M. Jacob, Nucl. Phys. **B238**, 221 (1984).

[3]UA1 Collaboration, G. Arnison *et al.*, Phys. Lett. **122B**, 103; **126B**, 398 (1983); UA2 Collaboration, M. Banner *et al., ibid.* **122B**, 476 (1983); P. Bagnaia *et al., ibid.* **129B**, 130 (1983).

[4]V. Barger, H. Baer, A. D. Martin, and R. J. N. Phillips, Phys. Rev. D **29**, 887 (1984); V. Barger, H. Baer, K. Hagiwara, A. D. Martin, and R. J. N. Phillips, *ibid.* **29**, 1923 (1984).

[5]V. Barger, H. Baer, A. D. Martin, E. W. N. Glover, and R. J. N. Phillips, Phys. Lett. **133B**, 449 (1983); Phys. Rev. D **29**, 2020 (1984); D. Cline and C. Rubbia, Phys. Lett. **127B**, 277 (1983); S. Gottlieb and T. Weiler, Phys. Rev. D **29**, 2005 (1984).

[6]V. Barger, W.-Y. Keung, and R. J. N. Phillips, Phys. Lett. B (to be published); R. Thun, *ibid.* **134B**, 459 (1984).

[7]M. Veltman, Nucl. Phys. **B123**, 89 (1977); M. B. Einhorn, D. R. T. Jones, and M. Veltman, *ibid.* **B191**, 146 (1981).

[8]J. Kim, P. Langacker, M. Levine, and H. Williams, Rev. Mod. Phys **53**, 211 (1980). The values quoted are from the updated analysis in W. J. Marciano and A. Sirlin, Phys. Rev. D **29**, 245 (1984).

[9]W. J. Marciano and A. Sirlin, Phys. Rev. D **22**, 2695 (1980); F. Antonelli, M. Consoli, and G. Corbo, Phys. Lett. **91B**, 90 (1980); M. Veltman, *ibid.* **91B**, 95 (1980).

[10]M. S. Chanowitz, M. A. Furman, and I. Hinchliffe, Phys. Lett. **78B**, 285 (1978); Nucl. Phys. **B153**, 402 (1979).

[11]P. Q. Hung, Phys. Rev. Lett. **42**, 875 (1979); H. D. Politzer and S. Wolfram, *ibid.* **82B**, 242 (1979); R. A. Flores and M. Sher, Phys. Rev. D **27**, 1679 (1983).

[12]N. Cabibbo, L. Maiani, A. Parisi, and R. Petronzio, Nucl. Phys. **B158**, 295 (1979); H. Komatsu, Prog. Theor. Phys. **65**, 779 (1981); J. Oliensis and M. Fishler, Phys. Rev. D **28**, 194 (1983).

[13]B. Pendleton and G. G. Ross, Phys. Lett. **98B**, 291 (1981); C. Hill, Phys. Rev. D **24**, 691 (1981); E. A. Paschos, Madison Report No. MAD/PH/162, 1984 (unpublished); see also the last paper in Ref. 12.

[14]See, e.g., the review by J. Ellis, CERN Report No. TH-3616, 1983 (unpublished) and references therein.

[15]L. Wolfenstein, Phys. Rev. Lett. **51**, 1945 (1983); W.-Y. Keung, and L. L. Chau, Phys. Rev. D **29**, 592 (1984); I. I. Bigi and A. I. Sanda, Fermilab Report No. PUB 83-74-THY (unpublished); T. Brown and S. Pakvasa, Univ. of Hawaii Report No. UH-511-514-84 (unpublished); E. Paschos and U. Turke, Santa Barbara Report No. NSF-ITP-83-168 (unpublished); F. J. Gilman and J. S. Hagelin, Phys. Lett. **133B**, 443 (1983); K. Kleinknecht and B. Renk, Z. Phys. C **16**, 7 (1982).

[16]E. Fernandez *et al.*, Phys. Rev. Lett. **51**, 1022 (1983); N. S. Lockyer *et al., ibid.* **51**, 1316 (1983).

[17]B. Gittleman, talk at Physics of 21st Century Conference, Tuscon, 1983 (unpublished).

[18]We note in passing that the permutation-symmetry model of Y. Yamanaka, H. Sugawara, and S. Pakvasa, Phys. Rev. D **25**, 1895 (1982) gives a symmetric three-generation mixing matrix; this model has no *CP*-violating phase in the quark sector, however. See also S. Pakvasa, H. Sugawara, and S. F. Tuan, Z. Phys. C **4**, 53 (1980).

[19]K. Fujikawa, Prog. Theor. Phys. **61**, 1186 (1979); T. Rizzo, Phys. Rev. D **23**, 1987 (1981).

[20]S. Pakvasa, H. Sugawara, and S. F. Tuan, Z. Phys. C **4**, 53 (1980).

[21]E. Golowich and T. C. Yang, Phys. Lett. **80B**, 245 (1979); D. R. T. Jones, G. L. Kane, and J. P. Leveille, Phys. Rev. D **24**, 2990 (1981).

[22]*Proceedings of the 1982 DPF Summer Study on Elementary Particle Physics and Future Facilities, Snowmass, Colorado,* edited by R. Donaldson, R. Gustafson, and F. Paige (Fermilab, Batavia, Illinois, 1982); Fermilab proposal for a dedicated collider, 1983 (unpublished).

[23]J. F. Owens and E. Reya, Phys. Rev. D **17**, 3003 (1978); D. W. Duke and J. F. Owens, *ibid,* **30**, 49 (1984).

[24]See, e.g., F. Halzen, in *Proceedings of the 21st International Conference on High Energy Physics, Paris, 1982,* edited by P. Petiau and M. Porneuf [J. Phys. (Paris) Colloq. **43**, C3-381 (1982)].

[25]V. Barger, F. Halzen, and W.-Y. Keung, Phys. Rev. D **24**, 1428 (1981); **25**, 112 (1982).

[26]B. L. Combridge, Nucl. Phys. **B151**, 429 (1979).

[27]R. Odorico, in *Proton-Antiproton Collider Physics—1981,* proceedings of the Workshop, Madison, Wisconsin, edited by V. Barger, D. Cline, and F. Halzen (AIP, New York, 1982), p. 100.

[28]F. Paige, talk at Gordon Conference, 1983 (unpublished); R. Odorico, CERN Report No. TH.3678 (unpublished).

[29]V. Barger, A. D. Martin, and R. J. N. Phillips, Z. Phys. C **21**, 99 (1983).

[30]R. Marshall, Rutherford Appleton Report No. RAL-84-002 (unpublished).

[31]V. Barger and R. J. N. Phillips, Wisconsin Report No. MAD/PH/160 (1984).

[32]J. Gunion, Phys. Lett. **88B**, 150 (1979); R. Horgan and M.

Jacob, *ibid.* **107B**, 395 (1981).
[33]R. W. Brown and K. O. Mikaelian, Phys. Rev. D **19**, 922 (1979).
[34]R. Kinnunen, in *Proton-Antiproton Collider Physics—1981* (Ref. 27), p. 236; R. Brown *ibid.*, p. 251; B. Humpert, Phys. Lett. **135B**, 179 (1984).
[35]J. Stroughair and C. L. Bilchak, Case—Western Reserve Report No. CWRV-83-4 (unpublished), K. J. F. Gaemers and G. J. Gounaris, Z. Phys. C **1**, 259 (1979).
[36]V. Barger, Wisconsin Report No. MAD/PH/165, 1984 (unpublished).